Paleomagnetic Evidence for a Stationary Marion Hotspot: Additional Paleomagnetic Data from Madagascar

J.G. Meert and Endale Tamrat

Department of Geological Sciences, University of Florida, 241 Williamson Hall,
Gainesville, FL 32611 (jmeert@geology.ufl.edu)

Gondwana Research Submission

Abstract

The island of Madagascar experienced widespread magmatism at ca. 90 Ma due to its interaction with the Marion hotspot. Previous paleomagnetic data from igneous rocks in the southwestern and northwestern regions of the island indicated that the Marion hotspot has remain fixed for the past 90 Ma. We report paleomagnetic data from northeastern Madagascar (d’Analava Complex). Samples were collected from basalts, rhyolites, gabbros and a dolerite dyke. Sixty samples from 5 sites yield a paleomagnetic pole at 66.7° S, 43.5° E (A95=10.7°) and a grand mean pole (GMP) calculated from 10 different studies covering the entire island of Madagascar falls at 68.9° S, 49.0° E (A95=4.4°). This pole translates to a paleolatitude for the Volcan de l’Androy (focal point of the hotspot) at 45.2° S +6°/-5° compared to the current location of the Marion hotspot at ~46° S. Our results confirm, and expand upon, previous studies that argue for the fixity of the Marion hotspot for the past 90 Ma.

Keywords: Marion hotspot, paleomagnetism, Madagascar, Cretaceous, paleolatitude

Introduction

The breakup of the eastern Gondwana continent within Pangea commenced in mid-Jurassic times with the initiation of rifting between the combined Madagascar-India blocks at around 165 Ma (see Coffin and Rabinowitz, 1988 Figure 1a). Torsvik et al. (1998) argued that following the cessation of seafloor spreading between Africa and Madagascar at 130 Ma, widespread magmatism ensued due to the interaction of Madagascar and the Marion hotspot. They further argued that the paleomagnetic data were consistent with the fixity of the Marion hotspot for the last 90 Ma. IN a followup study, Riisager et al. (2001) collected 144 drill cores from 15 sites along the northwestern part of the island of Madagascar (Figure 1b) and published a detailed paleomagnetic pole for the Late Cretaceous of Madagascar with coordinates at 67.8 S, 48.5 E). Their study also agreed with the conclusions of Torsvik et al. (1998) regarding the fixity of the Marion hotspot. Since the igneous activity took place during the Cretaceous Normal Superchron (CNS), Riisager et al. (2001) also provided an estimate for the intensity of the paleofield and an analysis of paleosecular variation. The conclusion was that paleosecular variation recorded in these eruptive products was somewhat lower than expected, but not statistically significant.

In an effort to complete the island-wide sampling of these Late Cretaceous eruptive products, we collected 5 additional paleomagnetic sites from northeastern Madagascar where the d'Analava gabbroic Complex (91.6 ± 3 Ma; Torsvik et al., 1998) is thought represent one of the feeder magma chambers to the Late Cretaceous volcanic rocks. We report the results in this paper and derive a grand mean pole (GMP) for the island of Madagascar.

Sampling Procedure

Figure 1b shows the locations of paleomagnetic sampling sites in the Late Cretaceous igneous rocks and Table 1 gives the GPS coordinates of the sampling locations. We collected 70 samples from 5 sites. One of our sites included a doleritic dike that intruded country rocks thought to have undergone metamorphism during the Late Neoproterozoic (Meert et al., in prep). Two sites were from basalts, one in rhyolites and the last site in the D'Analava gabbroic complex.

All samples were drilled in the field using a gasoline-powered drill and oriented using both magnetic and sun compasses. The samples were then cut into specimens at the University of Florida. Individual samples were then stepwise treated using thermal (60 minutes at each temperature level) or alternating field demagnetization and a treatment sequence was selected that resulted in the clearest separation of individual vector components. All samples were stored in a μ-metal shield for one month prior to measurement. Alternating field demagnetization was conducted using a home-built AF-demagnetizer able to reach peak fields of 140 mT and thermal demagnetization was conducted using an ASC-Scientific thermal demagnetizer. Samples were measured in a Molspin® spinner magnetometer.

Curie temperature runs were conducted on powdered samples using the KLY-3S susceptibility bridge adapted with a CS-3 heating unit (AGICO). Susceptibility measurements are made incrementally during the heating and cooling of the samples. In an effort to minimize chemical alteration of the samples during heating, a constant flow of high purity argon gas was pumped into the system at a constant flow rate (100 ml min^{-1}).

Results

d'Analava Gabbro

A total of 8 samples were collected from the gabbroic body at d'Analava (13.57 S; 49.98 E). Figure 2 (a-f) shows typical demagnetization behavior of the gabbro samples using both alternating field (figure 2a,b,c) and thermal demagnetization (Fig 2,d,e,f). Alternating field demagnetization up to peak fields of 140 mT was usually only able to remove just over 50% of the natural remanent magnetization (NRM) in most samples (Fig 2a,b,c). Thermal demagnetization (Fig 2d,e,f) resulted in a much clearer demagnetization trajectory with a discrete unblocking temperature range between 500-575° C and the remaining samples were thermally treated. The overall mean direction (after cleaning) was declination (D=7.8°) and inclination (I=-49° k=198 and α95=3.9°, figure 2g) with a resultant virtual geomagnetic pole (VGP) at 72.5° S, 26.8° E (dp=3.4°; dm=5.1°). Given that Madagascar was in the southern hemisphere during the emplacement of the gabbro, the polarity of the samples is all normal. The age of the d'Analava complex was reported by Torsvik et al. (1998) at 91.6 ± 3 Ma. Due to the discrete unblocking temperature spectra and the relatively high coercivity of the samples, we conclude that low-Ti magnetite is the main carrier. Curie temperature runs (fig 2h) also show a very sharp drop in susceptibility at 578° C during the heating phase and some slight alteration of the magnetite grains upon cooling. These are both consistent with relatively low-Ti magnetite as the dominant carrier in the samples.

Cretaceous Basalts

A total of 31 samples were collected from the basaltic flows at 2 different sites (14.27 S; 50.16 E and 14.45 S, 50.17 E). Figure 3 (a-f) shows typical demagnetization behavior of the basaltic samples using both alternating field (figure 3a,b,c) and thermal demagnetization (Fig 3,d,e,f). Alternating field demagnetization up to peak fields of 100 mT was usually able to remove more than 80% of the natural remanent magnetization (NRM) in most samples (Fig 3a,b,c). Thermal demagnetization (Fig 3d,e,f) resulted in a clean demagnetization trajectory with a distributed unblocking range from ~200-525° C. Half of the remaining samples were treated thermally and the other half using alternating field. The overall mean direction (after cleaning) for the first basalt site (CA-samples) was declination (D=7.2°) and inclination (I=-50°) with k=157 and $\alpha 95=2.5°$ with a resultant virtual geomagnetic pole (VGP) at 75.5° S, 26.1° E (dp=2.1°; dm=3.3°). These basalts are thought to be genetically related to the 91.6 Ma d'Analava gabbro complex. Due to the relatively low and distributed unblocking temperature spectra and the relatively low coercivity of the samples, we conclude that the carrier of the magnetization in the basalts are titanomagnetites. Curie temperature runs (fig 3h) also show a very sharp drop in susceptibility at 578° C during the heating phase and some slight alteration of the magnetite grains upon cooling.

Cretaceous Rhyolite

A total of 11 samples were collected from a small outcrop of rhyolite outside of the town of Sambava, Madagascar (14.20 S; 50.05 E). Figure 4 (a-f) shows typical demagnetization behavior of the rhyolite samples using both alternating field (figure 4a,b,c) and thermal demagnetization (Fig 4,d,e,f). Alternating field demagnetization up to peak fields of 140 mT was usually only able to remove just over 50% of the natural remanent magnetization (NRM) in most samples (Fig 4a,b,c). Thermal demagnetization (Fig 4d,e,f) resulted in a slightly better demagnetization trajectory with distributed unblocking temperatures range between 300-590° C, but heating to 590° C did not completely remove the magnetization. Several samples were heated to 690° C but their behavior became erratic at temperatures above 600°. Half of the remaining samples were treated thermally and the other half using alternating field. The overall mean direction (after cleaning) was declination (D=1.5°) and inclination (I=-67.1° k=81 and $\alpha95$=5.1°, figure 4g) with a resultant virtual geomagnetic pole (VGP) at 54.4° S, 48.4° E (dp=7.0°; dm=8.5°). The age of the rhyolites are also thought to be related to magmatic activity associated with the 91.6 Ma d'Analava complex (See Torsvik et al., 1998). Due to the discrete unblocking temperature spectra and the relatively high coercivity of the samples, we conclude that low-Ti magnetite is the main carrier.

Cretaceous Dike

A 6.6 meter wide dike located along the Milanoa River (13.64° S; 49.76° E) intruded previously undated high grade metamorphic rocks. The dike shows very sharp chilled margins consistent with emplacement into relatively cool country rock. ^{40}Ar/^{39}Ar work on the same metamorphic rocks (4 kilometers south; Meert et al., in prep) yield plateau ages of 562 ± 5 Ma. A total of 16 samples were taken from the dike and host rocks. Susceptibility measurements were made on each core using a Sapphire Instruments (SI-2B) bridge and plotted as a function of distance from the contact (Figure 5a). Susceptibility values are orders of magnitude higher in the dike and the country rock immediately adjacent to the dike than in the unbaked country rocks (figure 5b). Samples were treated using alternating field demagnetization and the results are shown in Figures 5c-h. Samples from the dike and country rock within ½ dike width of the margin are all of normal polarity although samples from the dike tend to be somewhat steeper in inclination than the baked host (see figures 5c,d compared to figures 5e-g). Samples from the unbaked host show consistent westerly-steeply down directions that are quite distinct from the dike and are consistent with early Cambrian poles from elsewhere in Madagascar (Figure 5h; Meert et al., 2001; Meert et al., 2003). This provides strong evidence for a positive baked contact test.

Discussion

A paleomagnetic pole calculated from these 5 sites falls at 66.7° S, 43.5° E (A95=10.7°). If we average our pole with the summary of paleomagnetic poles compiled by Riisager et al. (2001), we arrive at a Grand Mean Pole (Table 2; Figure 6) at 68.9° S, 49° E (A95=4.4°, Q=7). The supposed focal point of the Marion plume is hypothesized to be at 24.2° S, 46° E (Volcan de l"Androy). The paleolatitude calculated for this location using the Grand Mean Pole is $45.2°^{+6°}_{-5°}$. The present-day latitude of the Marion hotspot is ~46°S. Thus, our study completes the examination of Cretaceous volcanism from around the island with a sampling of the d'Analava complex in northeastern Madagascar and confirms earlier results arguing for the fixity of the Marion hotspot for the last 90 Ma (Figure 6; Torsvik et al., 1998; Riisager et al., 2001).

Acknowledgements: The authors wish to thank Chad Pullen for help in the field collecting paleomagnetic samples and Les Lezards de Tana for logistical assistance. This work is supported by the National Science Foundation EAR98-05306.

References

Andriamirado, C.R.A., 1971. Recherches paleomagnetiques sur Madagascar: resultats et interpretations dans le cadre de la dislocation de la partie orientale du Gondwana, Ph.D. thesis, University of Strasbourg, 202 pp.

Coffin, M.F. and Rabinowitz, P.D. 1988. Evolution of the conjugate East African-Madagascan margins and the western Somali Basin, Special Paper - Geological Society of America, vol.226, 78 pp.

Meert, J.G., Nedelec, A., Hall, C., Wingate, M. and Rakotondrazafy, M., 2001. Paleomagnetism, geochronology and tectonic implications of the Carion granite, central Madagascar, *Tectonophys*., 340, 1-21.

Meert, J.G., Nedelec, A., Hall, C., 2003. The stratoid granites of central Madagascar: Paleomagnetism and further age constraints on Neoproterozoic deformation, *Precam. Res*., 120, 101-129.

Riisager, J; Perrin, M; Riisager, P; Vandamme, D, 2001. Palaeomagnetic results and palaeointensity of Late Cretaceous Madagascan basalt, J. Afr. Earth Sci., 32, 503-518.

Storetvedt, K.M, Mitchell, J.G., Abranches, M.C., Maaloe, D, Robin, G. 1992. The coast parallel dolerite dykes of east Madagascar; age of intrusion, remagnetization and tectonic aspects, *J. Afr. Earth Sci*, 15, 237-249.

Torsvik, T H; Tucker, R D; Ashwal, L D; Eide, E A; Rakotosolofo, N A; de Wit, M J, 1998. Late Cretaceous magmatism in Madagascar; palaeomagnetic evidence for a stationary Marion hotspot, Earth Planet. Sci. Lett., 164, 221-232.

Figure Legends

Figure 1: (a) The supercontinent Pangea during the Middle Jurassic 175 Ma just prior to breakup. (b) The island of Madagascar showing locations of previous paleomagnetic studies (1-9) and this study (10) along with a generalized geological map (after Torsvik et al., 1998).

Figure 2: Paleomagnetic results from the 90 Ma d'Analava gabbro (a) alternating field demagnetization vector diagram for sample KG-10 (b) stereoplot of the demagnetization vectors for sample KG-10 (c) intensity decay plot for KG-10 (d) thermal demagnetization vector diagram for sample KG-7 (e) stereoplot of the demagnetization vectors for sample KG-7 (f) intensity decay plot of sample KG-7 (g) stereoplot of the mean direction obtained from the d'Analava gabbro samples and (h) curie temperature run of sample KG-4 indicating magnetite as the main magnetic mineral in the sample.

Figure 3: Paleomagnetic results from the 90 Ma d'Analava basalts (a) alternating field demagnetization vector diagram for sample Ca-9b (b) stereoplot of the demagnetization vectors for sample CA-9b (c) intensity decay plot for CA-9b (d) thermal demagnetization vector diagram for sample CA-11b (e) stereoplot of the demagnetization vectors for sample CA-11b (f) intensity decay plot of sample CA-11b (g) stereoplot of the mean direction obtained from the d'Analava basalt samples and (h) curie temperature run of sample KB-8 indicating magnetite and a secondary magnetic phase (pyrrhotite) as the main magnetic minerals in the sample.

Figure 4: Paleomagnetic results from the d'Analava rhyolites (a) alternating field demagnetization vector diagram for sample KR-1a (b) stereoplot of the demagnetization vectors for sample KR-1a (c) intensity decay plot for Kr-1a (d) thermal demagnetization vector diagram for sample KR-5a (e) stereoplot of the demagnetization vectors for sample KR-5a (f) intensity decay plot of sample KR-5a (g) stereoplot of the mean direction obtained from the d'Analava rhyolite samples.

Figure 5: Paleomagnetic results from the Milanoa dike and country rock (a) conceptual map showing the sampling locations of dike and country rock (b) plot of log susceptibility versus distance from the dike contact. (c) alternating field demagnetization diagram for dike sample DI-7 and a stereoplot of the vectors (d) alternating field demagnetization diagram for dike sample DI-5 and a stereoplot of the vectors (e) alternating field demagnetization diagram for country rock sample DI-9 and a stereoplot of the vectors (f) alternating field demagnetization diagram for country rock sample DI-10 and a stereoplot of the vectors(g) alternating field demagnetization diagram for country rock sample DI-12 and a stereoplot of the vectors and (h) alternating field demagnetization diagram for country rock sample DI-15 and a stereoplot of the vectors.

Figure 6: Compilation of previous paleomagnetic studies and location of the Grand Mean pole at 68.9° S, 49° E (A95=4.4°, Q=7). Also shown are the locations of the Marion hotspot and the Volcan d'Androy that is thought to be the focal point for the marion hotspot volcanic activity at ca. 90 Ma.

Table 1. Paleomagnetic Results

Site	Rock Type	Dec	Inc	k	α95	N	Plat	Plong	dp	dm
1-CA *14.27 S* *50.16 E*	Basalt	7.2	-50	157	2.5	21	75.5 S	26.1 E	2.1	3.3
2-KG *13.57 S* *49.98 E*	Gabbro	7.8	-49	198	3.9	8	72.5 S	26.8 E	3.4	5.1
3- DI *13.64 S* *49.76 E*	Dolerite+ Baked Host rock	2.1	-45.4	77	5.5	10	76.6 S	41.6 E	4.4	7.0
3-DI	*Unbaked*	*273.6*	*+68.8*	*81*	*10.2*	*4*	*8.6 S*	*11.5 E*	*14.7*	*17.3*
4-KR *14.20 S* *50.05 E*	Rhyolite	1.5	-67.1	81	5.1	11	54.4 S	48.4 E	7	8.5
5-KB *14.45 S* *50.17 E*	Basalt	355.6	-68.8	135	4.2	10	52.1 S	54.6 E	6	7.1
Overall		**3.6**	**-56.1**	**52**	**10.7**	**60**	**66.7 S**	**43.5 E**		

Notes: Dec=declination, Inc=inclination, k=kappa precision parameter (Fisher, 1953), α95= cone of 95% confidence (Fisher, 1953), N=number of samples used, Plat=latitude of the paleomagnetic pole, Plong=longitude of the paleomagnetic pole, dp,dm=cone of 95% confidence about the paleomagnetic pole in the co-latitude direction (dp) and at a right angle to the co-latitude direction (dm)

Table 2. Summary of Paleomagnetic Studies.

Location	**Pole Lat**	**Pole Long**	**A95**	**Reference**
1. Massif d’Androy	64 S	63 E	7.7	Andriamirado, 1971
2. SE Coast	65.8 S	35.6 E	4.4	Andriamirado, 1971
3. Mangoky-Anilahy	73.7 S	73.1 E	10	Andriamirado, 1971
4. Antanimena	66.1 S	79.7 E	4.9	Andriamirado, 1971
5. Mailaka	70.3 S	63.1 E	6.9	Andriamirado, 1971
6. SW Madagascar	76.8 S	68.2 E	2.4	Torsvik et al., 1998
7. Tamatave-1	60.2 S	32.1 E	2.8	Andriamirado, 1971
8. Tamtave-2	65.5 S	38 E	6.0	Storetvedt et al., 1992
9. Antanimena-Malaika	74 S	43.7 E	5.3	Riisager et al., 2001
10. D’Analava Complex	66.7 S	43.5 E	12	This study
Mean 1-10	**68.9 S**	**49.0 E**	**4.4**	**This compilation**

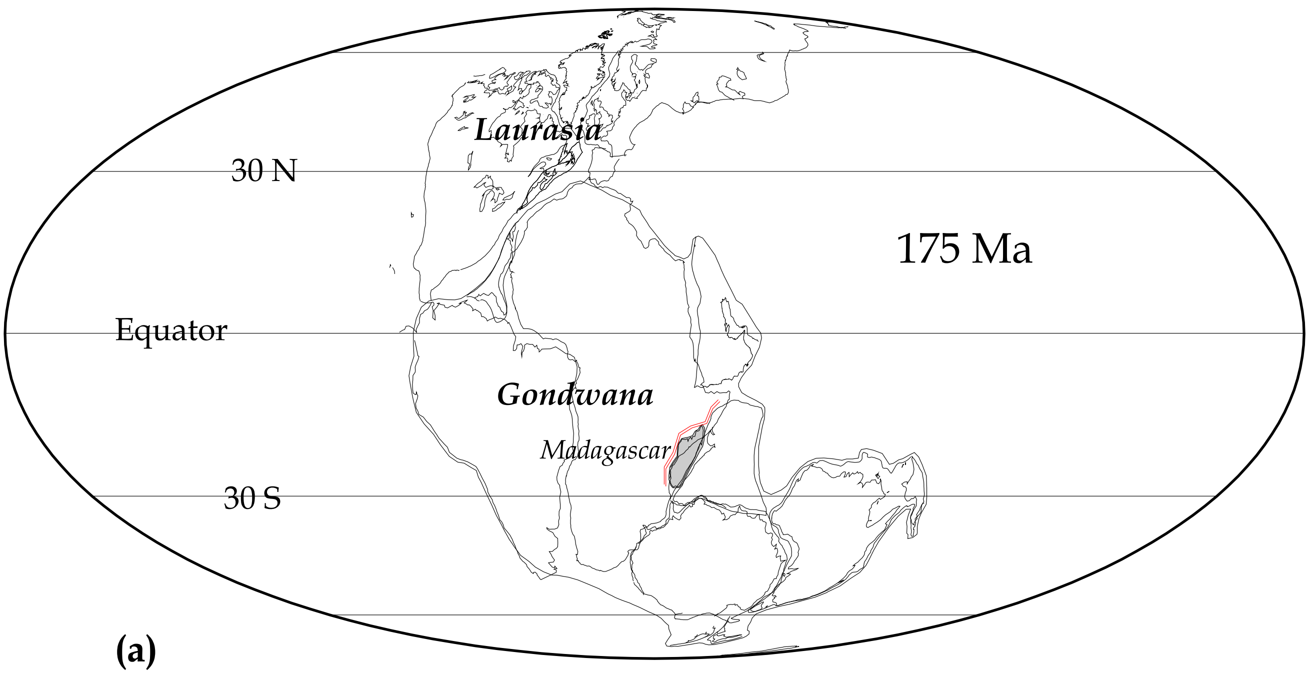
Laurasia
30 N
175 Ma
Equator
Gondwana
Madagascar
30 S

(a)

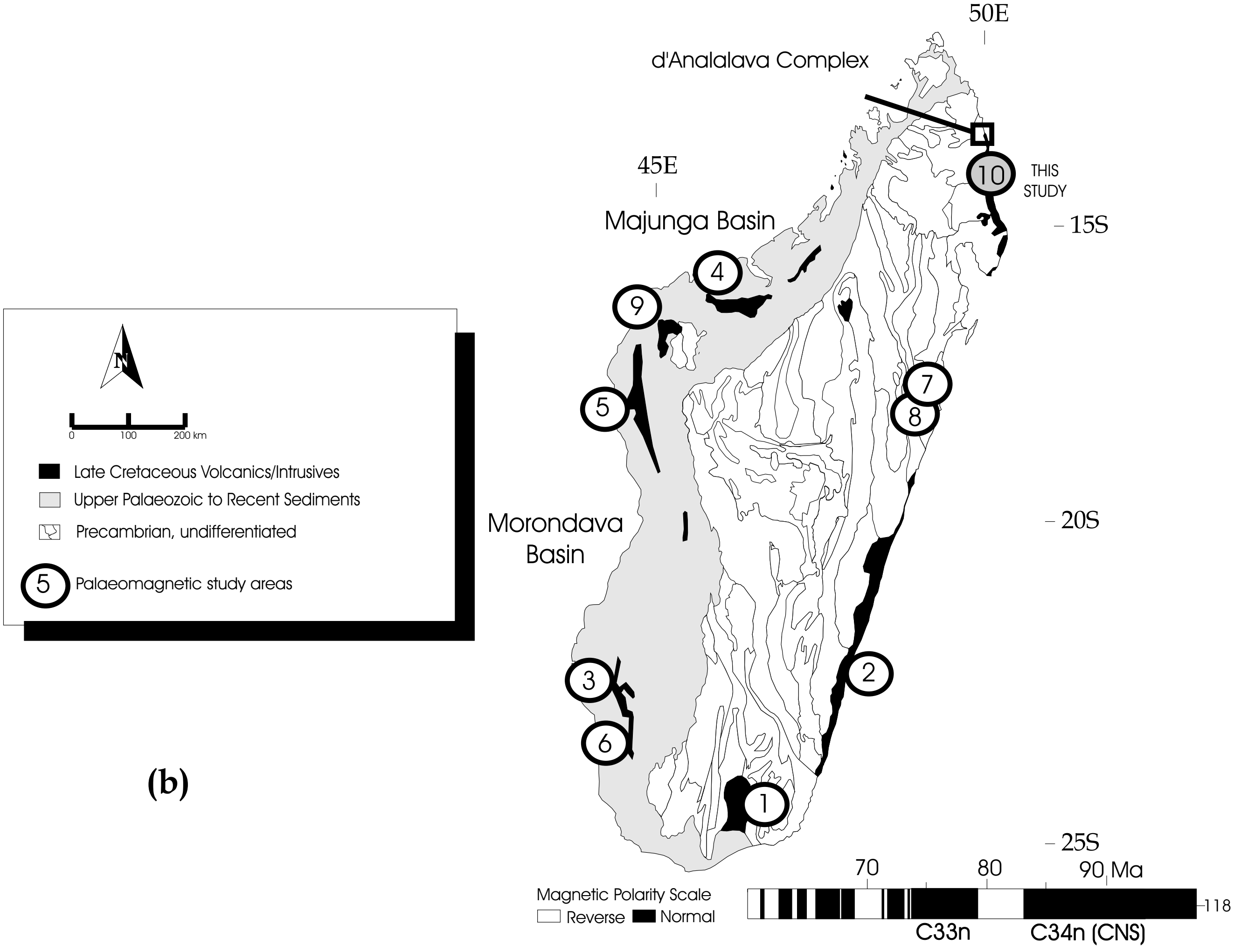
50E
d'Analalava Complex
10
THIS STUDY
45E
Majunga Basin
15S
4
9
N
0
100
200 km
5
7
8
Late Cretaceous Volcanics/Intrusives
Upper Palaeozoic to Recent Sediments
Precambrian, undifferentiated
5
Palaeomagnetic study areas
Morondava Basin
20S
3
2
6
1
25S
70
80
90 Ma
Magnetic Polarity Scale
Reverse
Normal
118
C33n
C34n (CNS)

(b)

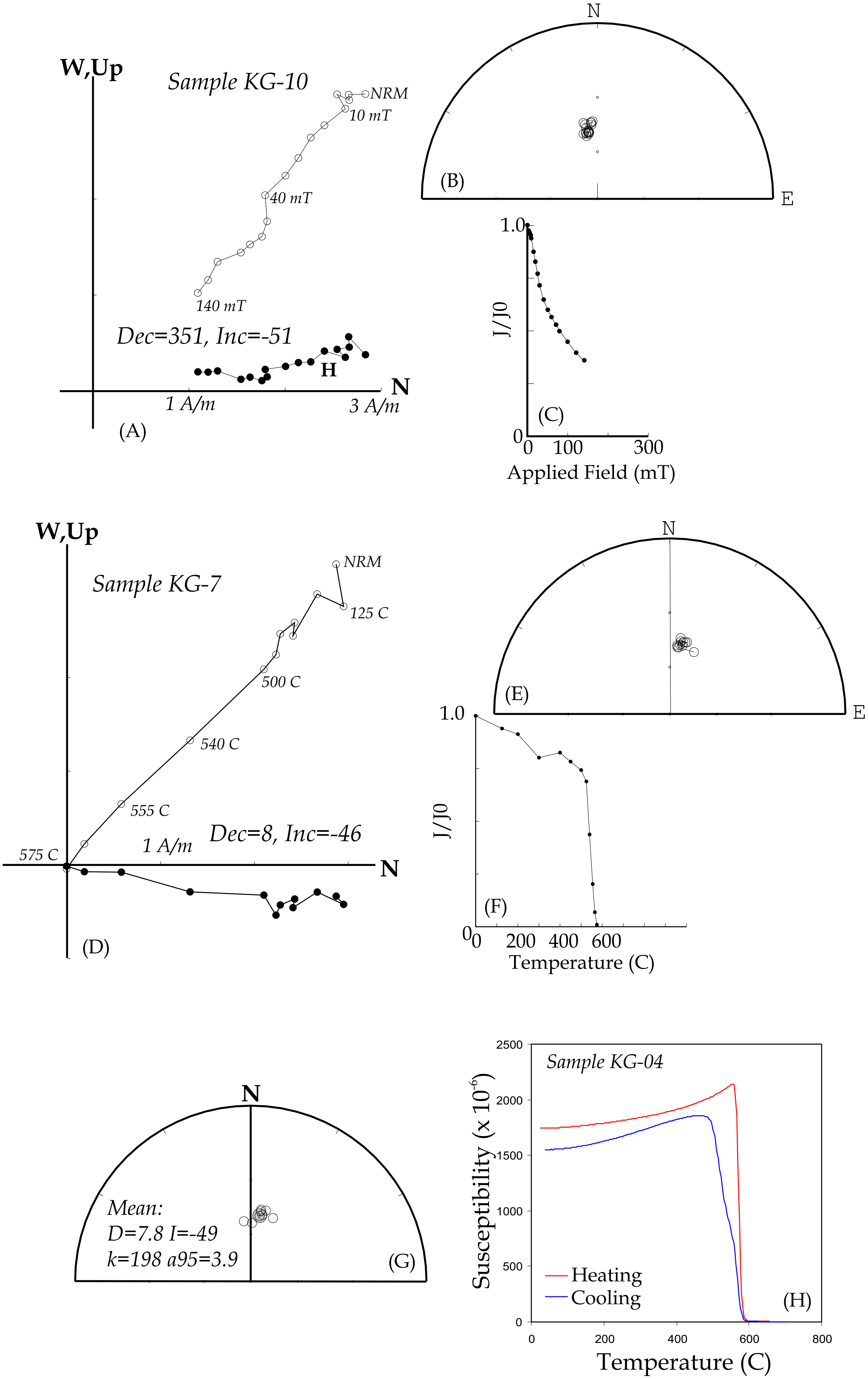
W,Up
Sample KG-10
NRM
10 mT
40 mT
140 mT
Dec=351, Inc=-51
H
N
1 A/m
3 A/m
(A)
N
E
(B)
1.0
J/J0
(C)
0
0
100
300
Applied Field (mT)
W,Up
Sample KG-7
NRM
125 C
500 C
540 C
555 C
575 C
1 A/m
Dec=8, Inc=-46
N
(D)
N
E
(E)
1.0
J/J0
(F)
0
0
200
400
600
Temperature (C)
N
Mean:
D=7.8 I=-49
k=198 a95=3.9
(G)
Sample KG-04
2500
2000
1500
1000
500
0
Susceptibility (x 10^-6)
Heating
Cooling
(H)
0
200
400
600
800
Temperature (C)

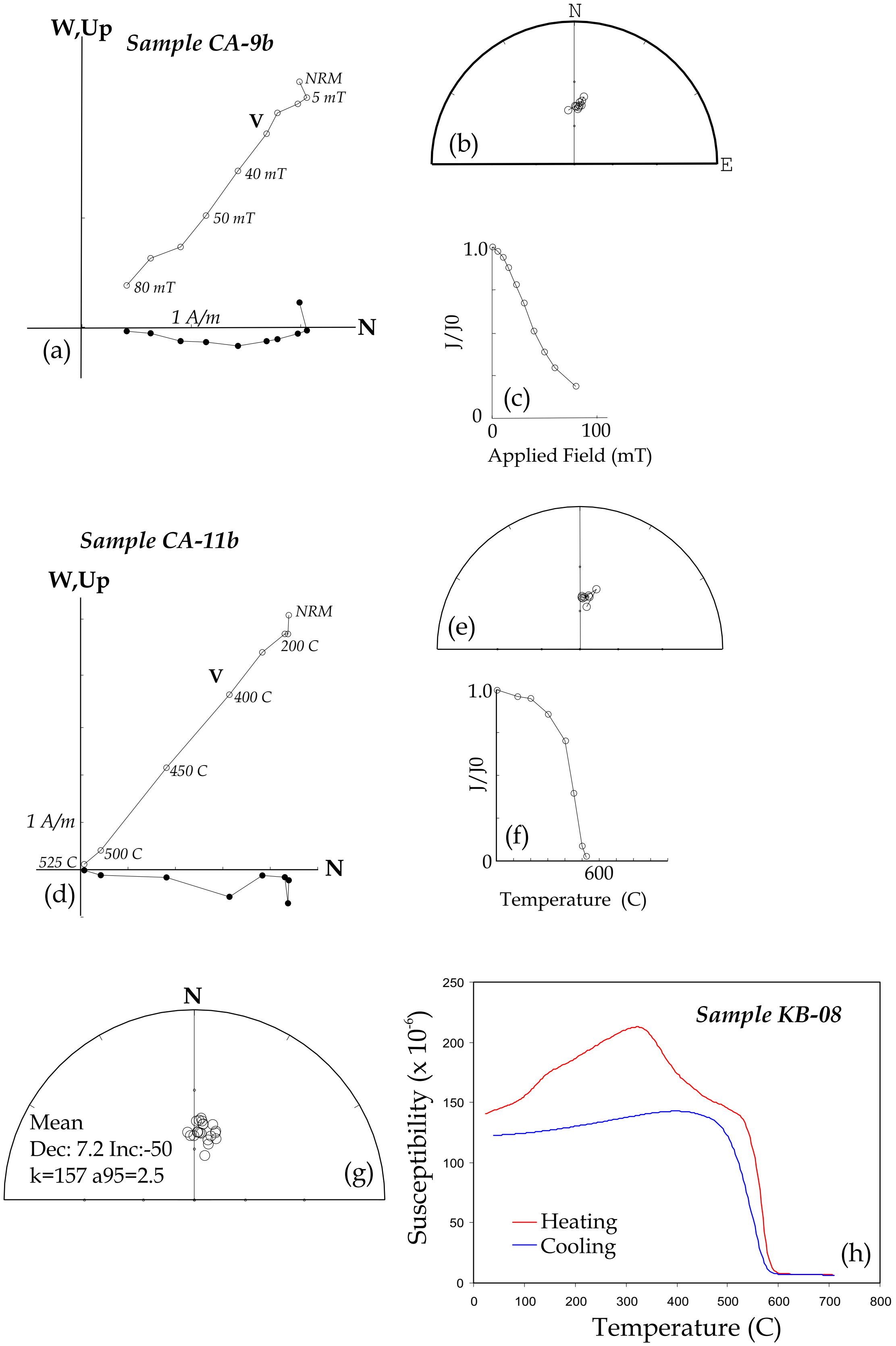
W,Up
Sample CA-9b
NRM
5 mT
V
40 mT
50 mT
80 mT
1 A/m
N
(a)
N
(b)
E
1.0
J/J0
(c)
0
0
100
Applied Field (mT)
Sample CA-11b
W,Up
NRM
200 C
V
400 C
450 C
1 A/m
500 C
525 C
N
(d)
(e)
1.0
J/J0
(f)
0
600
Temperature (C)
N
Mean
Dec: 7.2 Inc:-50
k=157 a95=2.5
(g)
250
200
150
100
50
0
Susceptibility (x 10^{-6})
Sample KB-08
Heating
Cooling
(h)
0
100
200
300
400
500
600
700
800
Temperature (C)

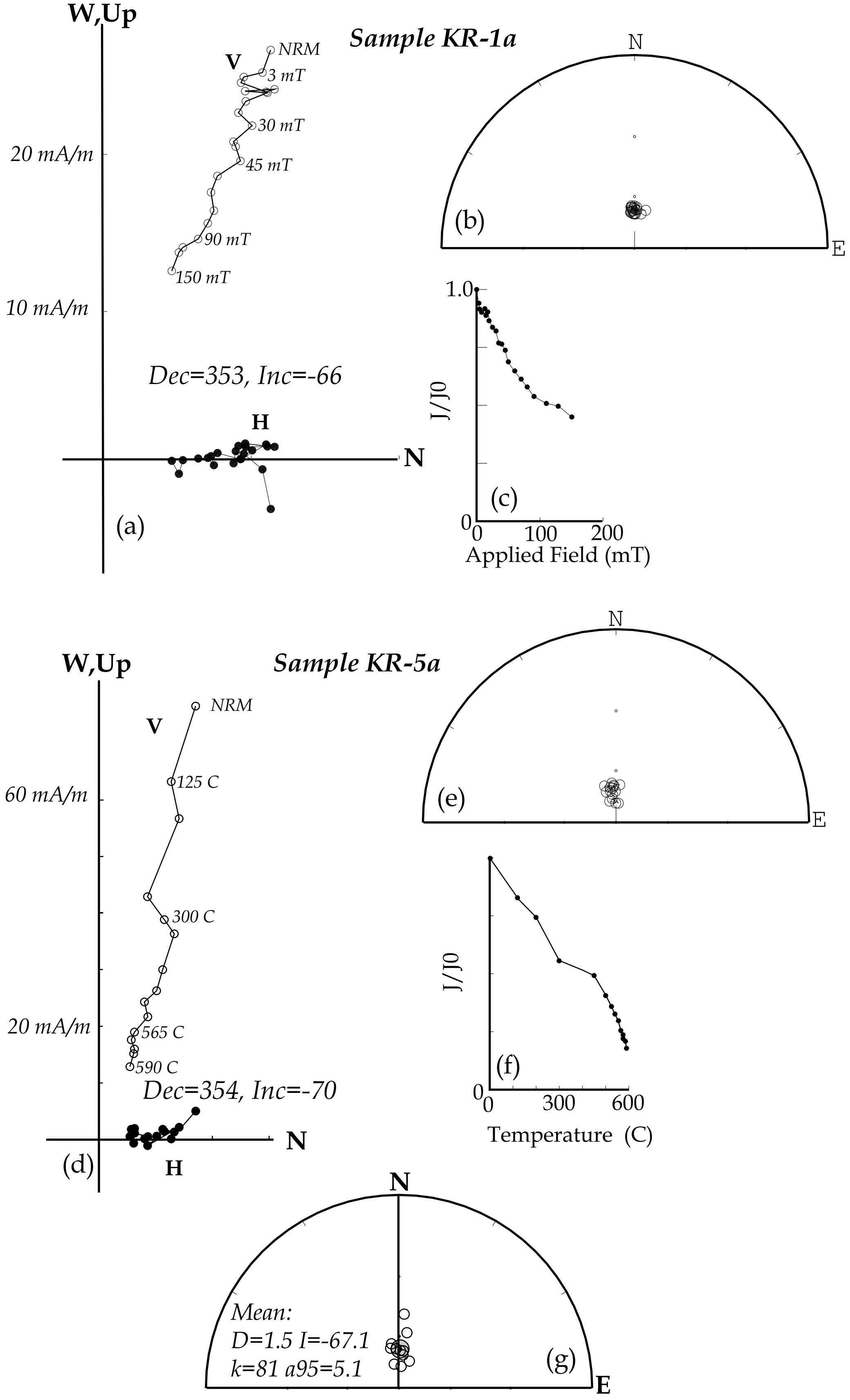
Sample KR-1a
W,Up
V
NRM
3 mT
30 mT
20 mA/m
45 mT
90 mT
150 mT
10 mA/m
Dec=353, Inc=-66
H
N
(a)
N
E
(b)
1.0
J/J0
(c)
0
0
100
200
Applied Field (mT)
Sample KR-5a
W,Up
V
NRM
125 C
60 mA/m
300 C
20 mA/m
565 C
590 C
Dec=354, Inc=-70
N
(d)
H
N
E
(e)
J/J0
(f)
0
0
300
600
Temperature (C)
N
Mean:
D=1.5 I=-67.1
k=81 a95=5.1
(g)
E

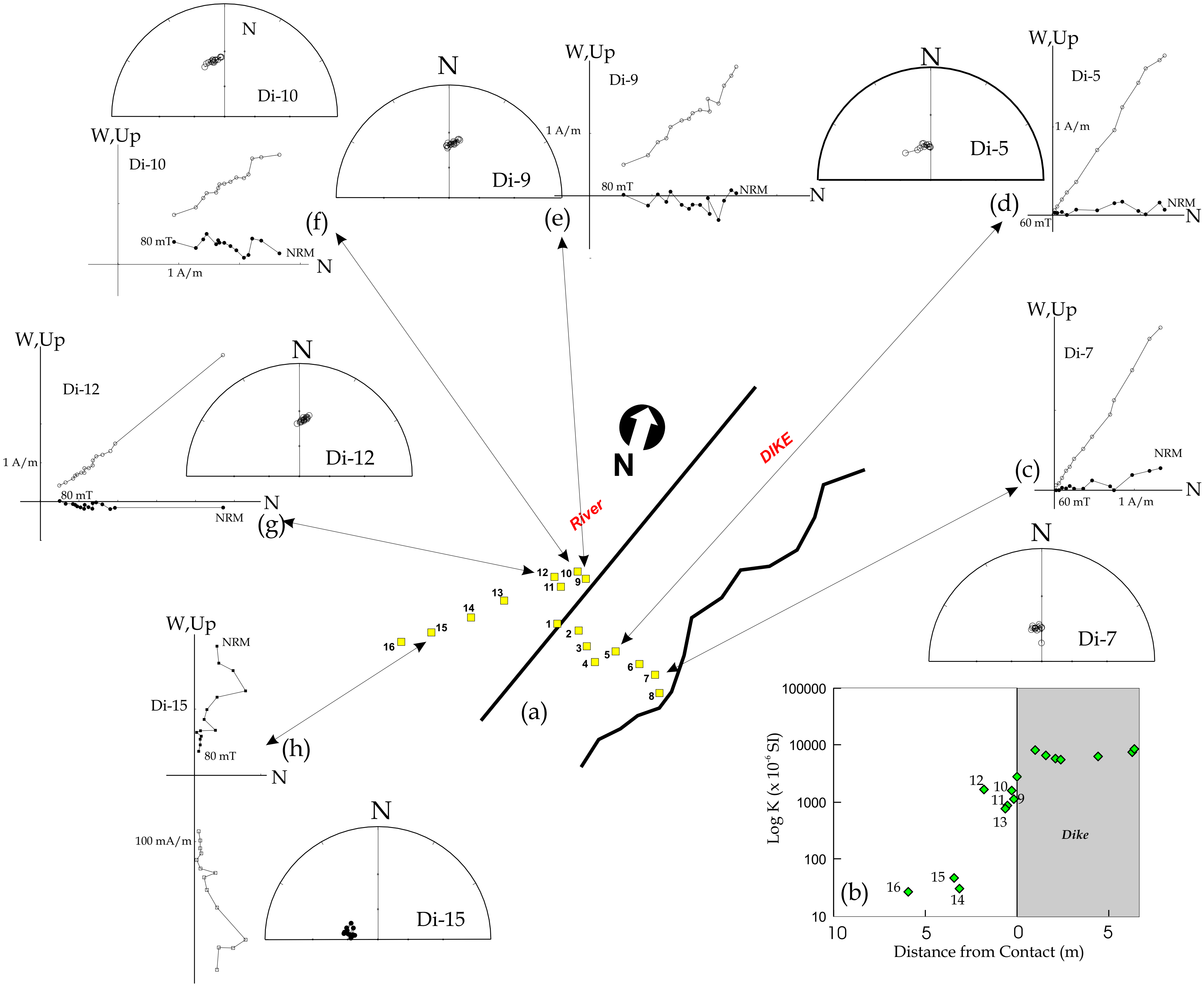
N
Di-10
W,Up
Di-10
80 mT
NRM
N
1 A/m
(f)
N
Di-9
W,Up
Di-9
1 A/m
80 mT
NRM
N
(e)
N
Di-5
W,Up
Di-5
1 A/m
NRM
60 mT
N
(d)
W,Up
Di-12
1 A/m
80 mT
NRM
N
(g)
N
Di-12
N
DIKE
River
12
10
9
11
13
14
1
2
3
5
4
6
7
8
15
16
(a)
W,Up
Di-7
NRM
(c)
60 mT
1 A/m
N
N
Di-7
W,Up
NRM
Di-15
80 mT
N
(h)
100 mA/m
N
Di-15
100000
10000
1000
100
10
Log K (x 10^-6 SI)
12
10
11
9
13
15
16
14
Dike
(b)
10
5
0
5
Distance from Contact (m)

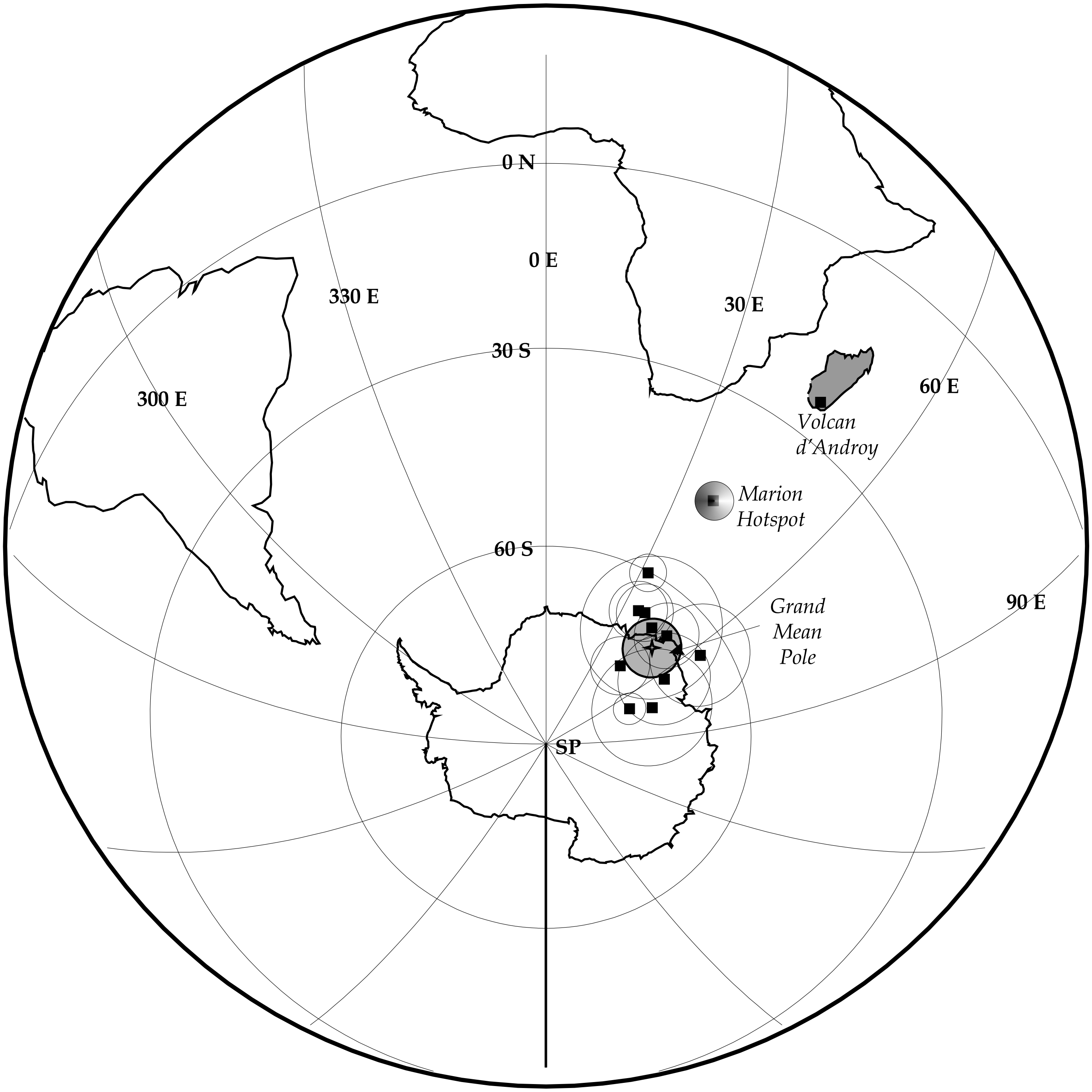
0 N
0 E
330 E
30 E
300 E
30 S
60 E
Volcan
d'Androy
Marion
Hotspot
60 S
Grand
Mean
Pole
90 E
SP